

ORIGINAL PAPER

L.S. Dubrovinsky · P. Lazor · S.K. Saxena
P. Häggkvist · H.-P. Weber · T. Le Bihan
D. Hausermann

Study of laser heated iron using third generation synchrotron X-ray radiation facility with imaging plate at high pressures

Received: 2 February 1998 / Accepted: 23 August 1998

Abstract Iron pressurized to 60 gigapascal (GPa) was heated with laser up to temperatures of over 2200 K. The structural changes were determined *in-situ* using third generation synchrotron X-ray source; the changes were recorded on an imaging plate with a monochromatic beam. The results strongly support the existence of a phase transformation of the hexagonal close-packed (hcp) structure to the new polymorph (β -phase of iron) at high pressure and temperature. We interpret the X-ray data as belonging to the double hexagonal close-packed (dhcp) structure distorted by stress due to laser heating.

Key words Iron · High pressure and temperature · Phase transition · Stress

Introduction

Ever since it was reported that iron may have new phase transformations at high pressure and temperature (Saxena et al. 1993a, 1995; Böhler 1993; Yoo et al. 1995), the confirmation and recognition of the new structure for iron has become crucial to all research related to the stability of iron phases in Earth's core. Although *in-situ* X-ray data have been presented before (Yoo et al. 1995;

Saxena et al. 1996; Dubrovinsky et al. 1997; Funamori et al. 1996; Shen et al. 1998; Andrault et al. 1997), it is necessary to study iron with the new synchrotrons (Andrault et al. 1997; Anderson 1997) such as the one we use in this study at ESRF (European Synchrotron Radiation Facility) with the fast scanning imaging plate. Earlier experiments (Yoo et al. 1995, 1996; Saxena et al. 1995, 1996; Funamori et al. 1996; Shen et al. 1998) were conducted with energy dispersive detectors using white radiation (except the one by Andrault et al. 1997). On heating, iron recrystallizes resulting in spotty lines which complicate the interpretation of the diffraction pattern. Our recent experiment (Dubrovinsky et al. 1997a) with CCD area detector and rotating anode X-ray source allowed us to partially overcome such problems. However we needed long data collection time (hours) and used a comparably large beam size (50–100 μm) with limited d-spacing range (up to 1.38 Å) which could hide some details of phase transition in iron.

The third generation synchrotrons permit the use of samples of much smaller size which can be heated thoroughly with little thermal gradient. This study differs from all our previous studies in several important ways. First, the X-ray data were collected as mentioned before with the new technique permitting us to obtain a full high resolution powder diffraction pattern from a small and thin iron sample. Second, we heated the sample with a laser to a high temperature and collected spectra *in-situ*. Third, because of the high resolution of the imaging plate and the availability of large portions of the Debye rings, we could recognize almost all the X-ray reflections necessary to characterise the crystal structure of the β -phase.

Methods

Experimental technique

Electrical heating is very stable, homogeneous and easy to regulate. But generation of temperatures higher than 1400 K at high pressure (above 50 GPa) is extremely difficult and the success of such

L.S. Dubrovinsky · P. Lazor · S.K. Saxena (✉) · P. Häggkvist
Institute of Earth Sciences,
Uppsala University,
S-752 36 Uppsala,
Sweden
Fax: +46 18 4712591
e-mail: leonid.dubrovinsky@geo.uu.se

H.P. Weber
Section de Physique,
Universite de Lausanne,
CH-1015 Lausanne,
Switzerland

T. Le Bihan · D. Hausermann
European Synchrotron Radiation Facility,
BP 220, Av des Martyrs,
F-38043 Grenoble,
France

experiments is a matter of chance. On the other hand, laser heating in the diamond-anvil cell (DAC) allows us to routinely reach temperatures as high as 2500 K at megabar pressure range. However, combination of laser heating and X-ray require special sample preparation. For example, we must use a proper thickness of the sample to minimize the axial (in loading direction) temperature gradient. Let us estimate the thickness of an iron foil which will limit the axial temperature gradient to 200 K when the sample is heated to 2500 K by Nd:YAG laser radiation from one side in a dielectric pressure medium (Fig. 1). (200 K corresponds to an uncertainty in temperature due to radial temperature gradients, fluctuations in laser power, uncertainties in emissivity at high pressure and temperature etc. (Lazor and Saxena 1996; Shen and Lasor 1996). As a first approximation we adopt the model suggested by Manga and Jeanloz (1997), but we consider two layers (Fig. 1). If heat transfer is dominated by axial conduction through the metal and dielectric layers (Li et al. 1996; Manga and Jeanloz 1997), then the temperature distribution within these layers satisfies the one-dimensional steady heat conduction equations with boundary conditions:

$$\begin{aligned} \frac{d}{dz} k_m(T) \frac{dT}{dz} &= 0, \quad T = T_m \text{ at } z = 0, \quad T = T_w \text{ at } z = \delta_m; \\ \frac{d}{dz} k_d(T) \frac{dT}{dz} &= 0, \quad T = T_w \text{ at } z = \delta_m, \quad T = T_0 \text{ at } z = \delta_m + \delta_d; \\ q_m &= q_d, \end{aligned} \quad (1)$$

where T is temperature, $k(T)$ is thermal conductivity, q is thermal heat flow, and indexes d and m denote respectively the metal and dielectric layers (see also Fig. 1). If we assume that thermal conductivity is inversely proportional to temperature (Touloukian and Ho 1971; Berman 1976; Li et al. 1996)

$$k(T) = \frac{\lambda}{T} \quad (2)$$

the system of Eq. (1) could be analytically solved:

$$\begin{aligned} T_m(z) &= T_w \left(\frac{T_m}{T_w} \right)^{(1-z/\delta_m)} \\ T_d(z) &= T_0 \left(\frac{T_w}{T_0} \right)^{(1-(z-\delta_m)/\delta_d)} \\ T_w &= (T_0^p T_m)^{\frac{1}{p+1}}, \quad p = \frac{\lambda_d \delta_m}{\lambda_m \delta_d} \end{aligned} \quad (3)$$

In a typical experimental set-up for laser heated DAC at high pressure, we can assume the thickness of the isolating dielectric

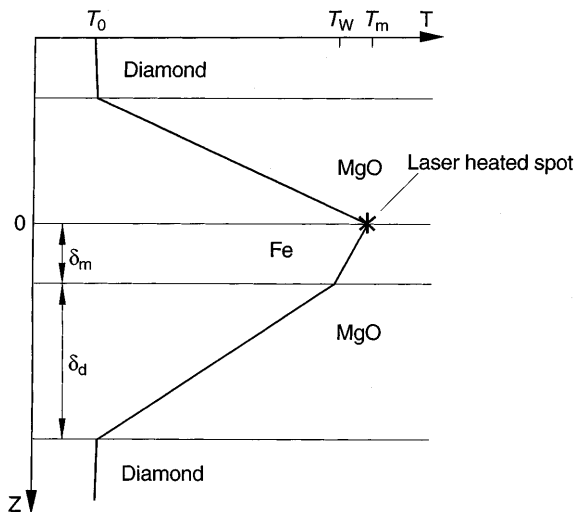


Fig. 1 Sketch of the temperature distribution across the thickness of the sample in laser-heated DAC

Fig. 2A–D Examples of images collected on ID30 beam line at ESRF with monochromatic 0.42 Å radiation with fast image plate during laser heating: **A** at room temperature and 61(1) GPa pressure determined using both ϵ -Fe and MgO equations of state; **B** at 1550(100) K; **C** at 2100(100) K; and **D** at 300 K and 25 GPa after recrystallization. All figures correspond to the same position of the laser and X-ray beam spots at the center of 30 μm in diameter and 3–4 μm initial thick iron foil. The monochromatic X-ray beam was focused using two single-electrode bimorph mirrors to a FWHM of 13*18 μm^2 and diameter of laser beam was approximately 35 μm . Inset belongs to part **C** and demonstrates that it is actually possible to resolve two iron spotty lines near the MgO (200) line

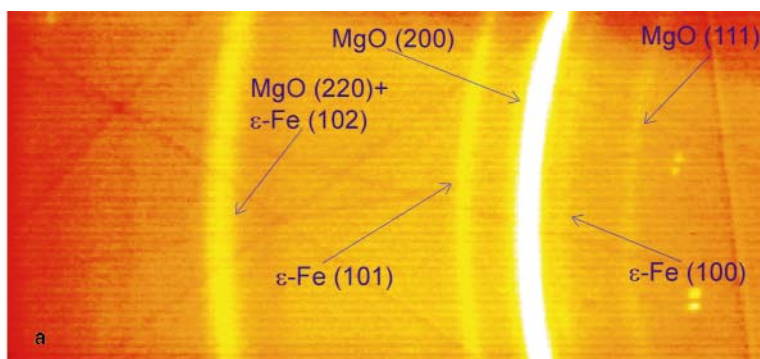
layers (periclase MgO, for example) $\delta_m \sim 5\text{--}10 \mu\text{m}$, and at high pressure and temperature $\lambda_m/\lambda_d \sim 8\text{--}15$ (Manga and Jeanloz 1997; Keeler and Mitchell 1969). We estimate the difference $T_m - T_w$ as $\sim 400\text{--}600$ K for a 5 μm thick iron foil and as 150–250 K for a 3 μm thick foil ($T_m = 2500$ K, $T_0 = 300$ K). Andrault et al. (1997) conducted *in situ* high- P , T experiments and reported that the laser heating of 5 μm thick iron foil in corundum pressure medium to a temperature of 2375 K caused the diffraction peaks to increase in width by 1.4 to 3.5 times (from 0.02–0.05 to 0.07° 2θ) in comparison to those at ambient condition for Si-standard. According to the equation of state of iron (Saxena et al. 1993b), it could be due to a temperature gradient of 400–500 K which is in perfect agreement with our estimations. Consequently, combination of laser heating and X-ray require very thin ($\sim 3 \mu\text{m}$) iron foil sample to avoid significant temperature gradients in the axial (loading) direction in the metal and, for the same reason, it should be perfectly isolated from diamonds requiring 20–25 μm thick layers of insulating material. If such a sample design is used, reflections due to the pressure medium will have a much higher intensity than that of the iron reflections. Therefore it is crucial that we use high intensity X-ray source such as the third generation synchrotron X-ray facilities at ESRF. At high temperature iron recrystallizes and instead of continuous diffraction rings, spotty pattern appears. Simple estimation shows, that at required thickness of the foil (3–4 μm) one can expect only 10–20 spots on the complete ring (Andrews 1955) at a beam size of 20 μm diameter and with sample-to-detector distance of 300 mm. Study of such samples is possible only in angle dispersive mode with area detectors. All these conditions are satisfied at the high-pressure study dedicated beam line ID30 at ESRF.

We drilled a 150 μm diameter hole in a steel gasket of an initial thickness of 200 μm which was indented to 80 μm . The sample was pure iron foil of an initial thickness of 5 μm which was further ground to a thickness of about 3 μm . This foil was embedded in pre-dried MgO powder (200 °C for six hours). The total diameter of the pressed iron sample was about 35 μm and the sample had become so thin as to be translucent in some spots in transmitted light. We estimate that the sample was about 3 μm thick which ensured a thorough heating of the sample with only little thermal gradient in the axial direction. The laser beam covered most of the sample.

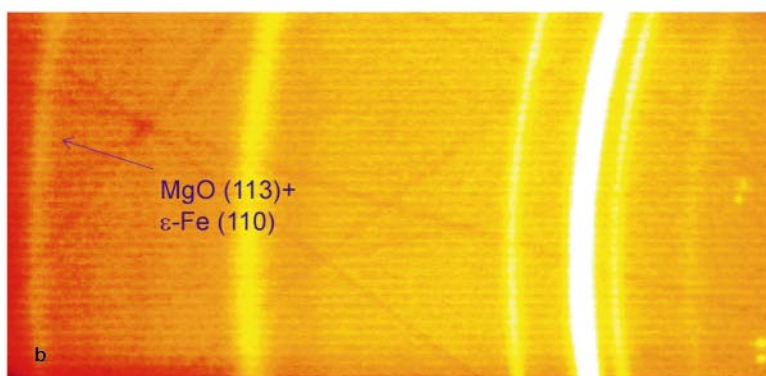
Laser heating system for synchrotron experiments

The sample in a diamond anvil cell is placed together with imaging and spectroradiometric system on a small board (30 × 60 cm) and the complete system is aligned and calibrated outside the hutch. All important positional changes are motorized and controlled from outside during the experiment. We used Nd:YAG laser (Quantronix, 110 W of continuous power) working in multimode which results in only small radial temperature gradient in the sample. The laser beam is focused by a lens (f.l. = 26 mm) down to a spot of about 35 μm entering the cell via the front slit at an angle of about 40°.

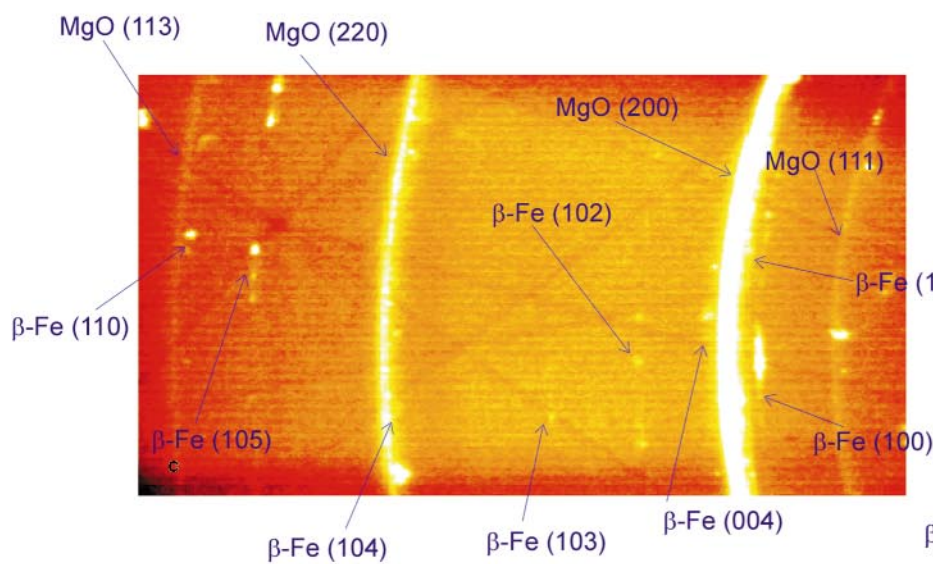
The temperature is determined by spectroradiometry. For each diffraction pattern temperature is measured before and after the acquisition which typically takes few minutes. During the acquisition



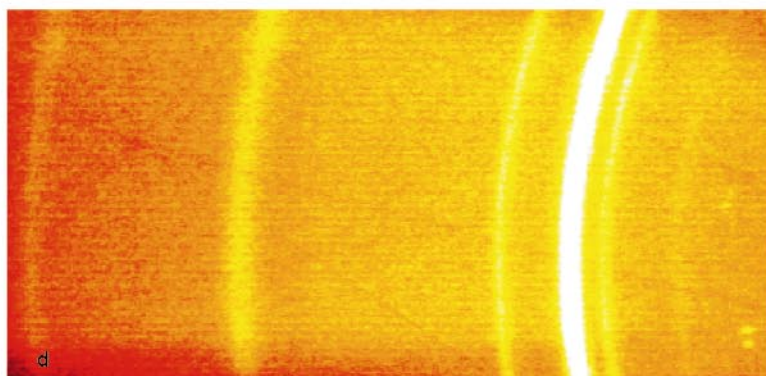
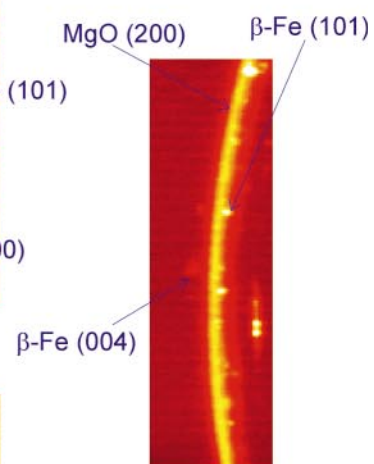
300 K, 61(1) GPa



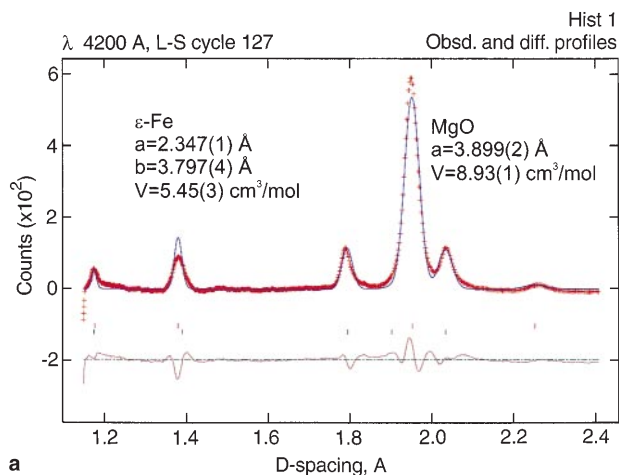
1550 (100) K



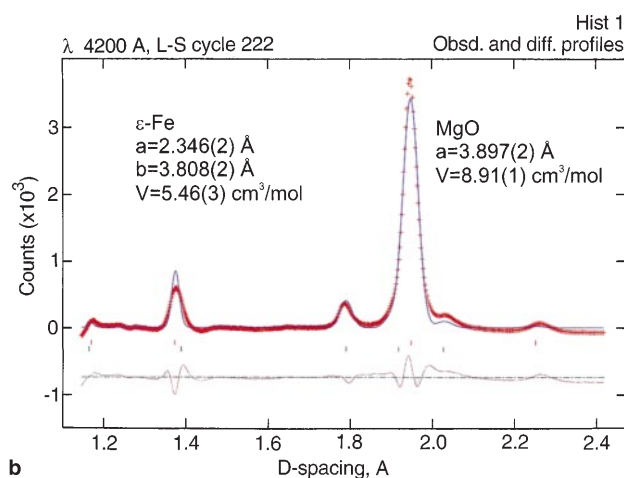
2100 (100) K



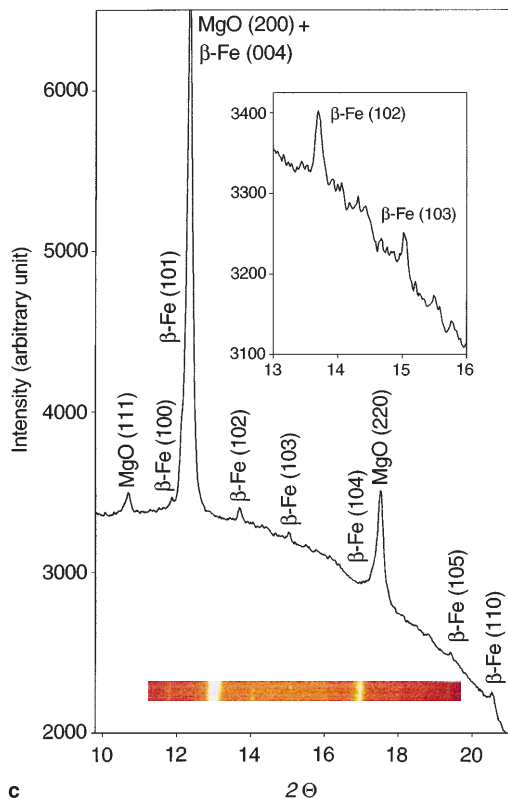
300 K, 25 GPa



a

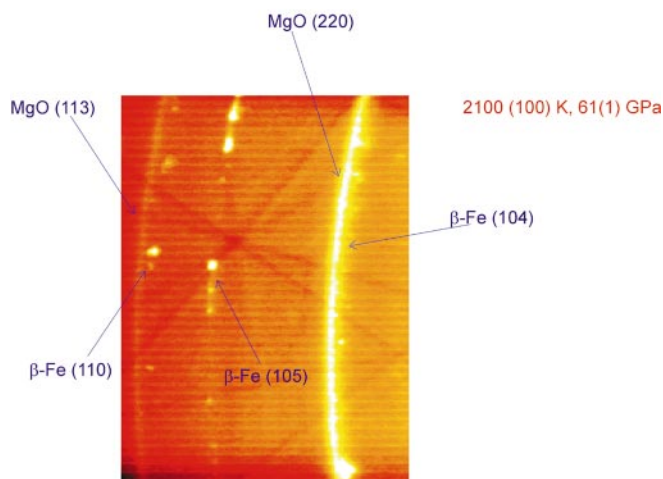
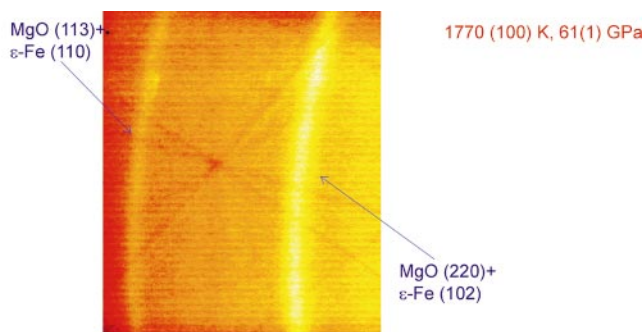


b



c

3



4

Fig. 3A–C Examples of analyzed integrated patterns of the spectrum collected at different temperatures: **A** at room temperature and 61(1) GPa; **B** same spot at 1550(100) K; and **C** the same spot at 2150(100) K. In cases **A** and **B** GSAS program package (Larson and Von Dreele 1994) was used. The *lower ticks* mark positions of Fe and *upper one* MgO pressure medium. Backgrounds for **A** and **B** were subtracted. While the temperature of the iron foil increased, the molar volume of the ϵ -Fe does not change. According to the thermal equation of state (Saxena et al. 1993b) it is possible if pressure in iron increased to 66 GPa. Assuming stress distribution model by Singh (1993), one can estimate the corresponding value of the uniaxial stress component t as 15 GPa. At high temperature **C** relative intensity, positions and shape of reflections is complicated due to complete recrystallization, strong preferred orientation effects and stresses and cannot be handled by GSAS program. (Moreover, generally speaking, each spotty lines or spots presented, for example, on Fig. 2C or on Fig. 3C (*inset*) could be produced by different crystallites in different orientation and, therefore, at completely different stress conditions. In such a case, not only structural analysis, but even determination of lattice parameter is doubtful). Colourful *inset* on **C** shows the part of image over which integration has been done. The d-spacings of the reflections of β -Fe shown on **C** are $d_{100} = 2.03$ Å, $d_{101} = 1.97$ Å, $d_{102} = 1.76$ Å, $d_{103} = 1.60$ Å, $d_{104} = 1.39$ Å, $d_{105} = 1.24$ Å, $d_{110} = 1.18$ Å



Fig. 4A, B Appearance of a new spotty line at $\approx 1.24 \text{ \AA}$ which we interpret as β -Fe (105) reflection. **A** Part of the image collected at 1770(100) K and 61(1) GPa (MgO cold pressure); **B** the same part at 2100(100) K. Iron recrystallized and transformed to β -Fe phase. New reflection marked as β -Fe (105) appeared

the imaging lens is remotely moved out of the path. The input pinhole of the spectrograph samples circular area of 4.5 \mu m on the sample. The CCD detector is shielded by lead plates. Melting point of Pt at 1 bar has been used for calibration of the system spectral response.

During laser heating, the cell temperature is actively stabilized with feedback to within few degrees by aluminum jacket with flowing water (Huber). We observe the surface of the diamond anvil cell close to the sample location under magnification in order to detect and compensate for any potential movement of the sample relative to the X-ray beam caused by thermal expansion of the cell during heating. We can observe any movement larger than 5 \mu m but with active cooling no action is usually needed. However, in a test run with cooling switched off, heating with high power for few minutes caused the temperature of the piston-cylinder to rise to almost $100 \text{ }^\circ\text{C}$ and active interference was needed to keep the sample spot in the X-ray beam.

Results and interpretations

The diffraction patterns for iron and MgO are shown in Figs. 2 and 3. In our analysis of the integrated X-ray spectra, we used the program GSAS (Larson and Von Dreele 1994) and PeakFit 4.0. At room temperature, the pressure was determined from the cell constants of hcp-Fe (ϵ) phase and from MgO (Fig. 3A, B).

Heating up to a temperature of 1700(100) K of the samples with pre-dried MgO did not produce any dramatic changes in the patterns. However, the intensity of (100) ϵ -Fe reflection increased relative to (101) reflection. We also noted a significant effect of stress which is different for iron and for MgO.

According to the general theory of the lattice strains in a specimen compressed nonhydrostatically in an opposed anvil device (Singh 1993; Singh and Balasingh 1994)

$$d_n(hkl) = d_h(hkl) \left[1 + t(1 - 3 \sin^2 \theta) f(h, k, l, S_{ij}) \right], \quad (4)$$

where indexes n and h correspond to nonhydrostatic and hydrostatic conditions respectively, t is uniaxial stress component, θ is Bragg diffraction angle, and $f(h, k, l, S_{ij})$ is a function depending on (hkl) and elastic compliance S_{ij} which was explicitly defined for cubic symmetry by Singh (1993) and for hexagonal symmetry by Singh and Balasingh (1994). As it follows from Eq. (4), if $t \neq 0$ lattice parameters calculated from different reflections will be different and this difference could be used to calculate value of t if elastic compliances are known (Funamori et al. 1994; Duffy et al. 1995).

For MgO, the difference between lattice parameter a calculated from (200) and (220) reflections, did not change with temperature ($\Delta = a_{220} - a_{200} = 0.009(2) \text{ \AA}$, which corresponds to a shear stress of approximately 5 GPa according to Duffy et al. 1995). For ϵ -Fe, the difference ($a_{100} - a_{110}$) increased from $0.012(3) \text{ \AA}$ to

$0.021(3) \text{ \AA}$. Thus the stresses in the Fe foil increased significantly with temperature. At least two factors help us to understand such behaviour; with increasing power of the laser, the temperature gradients (both radial and axial in the sample and pressure medium) increase which lead to increasing thermal stresses (Heinz 1994; Belonoshko and Dubrovinsky 1997) and with increasing temperature shear modulus of the metal decreases such that the same stress produces higher lattice strains.

At a temperature of 2100(100) K and pressure of 61 GPa iron recrystallized completely and several new spotty lines appeared (Figs. 2C, 3C, 4B and 4C). Those lines (for example, at 1.57 and 1.24 \AA) cannot be interpreted as ϵ - or γ -iron lines. New lines, that appeared in experiments with carefully dried MgO, could not be due to chemical reaction, because after experiment we lowered temperature and pressure to ambient condition, converted the iron to α phase and then pressurized it to 25 GPa (Fig. 2D), and all the additional lines disappeared. Moreover, we heated the same sample at 25 GPa, and transformed ϵ -Fe to γ -Fe at temperature higher than 1300 K and did not observe any new lines (or spots).

All the lines observed at high temperature could be interpreted as lines of the β -Fe with dhcp structure (Figs. 2, 3). These data demonstrate the advantage of the new ESRF high-pressure X-ray facility. We can clearly observe the lines (or rather spots) at 1.96 \AA and 1.57 \AA which correspond respectively to (004) and (103) reflections in our interpretation. For the first time we observe a quite strong spotty line at 1.24 \AA which could correspond to (105) reflection of the dhcp structure. All these lines could have been easily missed in experiments conducted in the energy dispersive mode. Only perfect spatial resolution of the imaging plate allows us to resolve (004), (101) lines of β -Fe and the highly intense (200) line of MgO (Fig. 2, inset).

The difference ($a_{100} - a_{110}$) for the β -Fe at 2100(100) K and 61 GPa (MgO cold pressure) is $0.030(2) \text{ \AA}$ as compared to $0.021(3) \text{ \AA}$ for ϵ -Fe at 1700 K; this result shows that stresses in the iron foil increased further with temperature. In DAC the principal stress in the load direction σ_3 is greater than the stress in the radial direction (in gasket plane) σ_1 and $t = \sigma_3 - \sigma_1$. In one-side laser heated DAC we can assume the same stress distribution model (Heinz 1986; Belonoshko and Dubrovinsky 1997). According to Singh and Balasingh (1994) for hexagonal sample under stress conditions

$$\begin{aligned} d_n(100) &= \frac{\sqrt{3}}{2} a_h \left[1 + \frac{t}{6\langle G \rangle_{hk0}} (3 \sin^2 \theta_{100} - 1) \right] \\ d_n(110) &= \frac{1}{2} a_h \left[1 + \frac{t}{6\langle G \rangle_{hk0}} (3 \sin^2 \theta_{110} - 1) \right] \end{aligned} \quad (5)$$

where $\langle G \rangle_{hk0}$ is average shear modulus in $(hk0)$ plane (Singh and Balasingh 1994) and a_h is lattice parameter at corresponding hydrostatic pressure.

For β -Fe using values of d-spacing for (100) and (110) reflections, we found the $t/\langle G \rangle_{hkl}$ to be 0.09(3). Elastic compliance at different pressures was theoretically calculated at 0 K by Söderlind et al. (1996). Using those data, one can estimate t as 20–30 GPa at our experimental conditions. Such high stresses affect the calculation of lattice parameters of β -Fe and introduce significant uncertainties. For example, for sample shown in Fig. 2 using all observed reflections we confirm that $a = 2.354(3)$ Å and $c = 7.787(88)$ Å. To account for the stress effect, we require knowledge of all stress components and elastic constants of the sample at given P - T conditions. Such information is not available yet. However, as a first approximation, we can apply a correction assuming that our sample is elastically isotropic. Using equations from Singh (1993) and Singh and Balasingh (1994), we calculated lattice parameters for β -Fe as $a = 2.322(2)$ Å and $c = 7.718(69)$ Å. The correction slightly improved quality of the fit, but the fit is still not good enough. Note, however, that a decrease in corrected values of the lattice parameters of the lattice parameters the hexagonal metals under deviatoric stress was predicted by Singh and Balasingh (1994). Our results show that β -Fe is significantly elastically anisotropic which is highly important for correct interpretation of the seismic anisotropy of the Earth's core.

Discussion

Based on the studies of quenched samples Saxena et al. (1995, 1996) suggested a dhcp structure for the new β -iron phase. Iron with dhcp structure was identified in the *in-situ* laser heating experiments of Yoo et al. (1995, 1996). However, this phase was considered as metastable (Yoo et al. 1995, 1996; Funamori et al. 1996) below 35 GPa and was not found at higher pressures. Shen et al. (1998) extended the possible range of metastable existence of iron with dhcp structure up to 60 GPa, but it was not detected *in situ*. Saxena and Dubrovinsky's (1997) analysis shows that this could be mainly due to poor resolution of energy dispersive spectrum and due to effects of preferred orientation, which hide superlattice reflection of dhcp structure. For example, Shen et al. (1998) at 68 GPa observed disappearance of reflections of MgO (used as pressure medium) at temperature above 2731 K. Because MgO at 68 GPa should melt at much higher temperature, the missing reflections could be due to low sensitivity of energy dispersive detector or due to recrystallization at high temperature. Experiments with electrically heated DAC at pressures up to 68 GPa in different pressure medium (Ar and corundum) confirm the phase transition ϵ to β iron with dhcp structure (Dubrovinsky et al. 1997, 1998b). Recently Andrault et al. (1997) conducted an *in-situ* X-ray study of heated iron at high pressure and found a structural transformation of ϵ (hexagonal close packed, hcp) iron to β to which they assigned an orthorhombic lattice. This new orthorhombic phase was found at almost the same P , T -

conditions as the dhcp-Fe (Dubrovinsky et al. 1997) and Andrault et al. (1997) believe that an orthorhombic structure should be used to correctly interpret all previous observations on phase transition of β -iron at pressure higher than 40 GPa. However, analysis done by Dubrovinsky et al. (1998a) demonstrate, that data by Andrault et al. (1997) could be affected by stresses and chemical reactions between iron and pressure medium.

Conclusions

We determined *in-situ* structural changes in heated iron using third generation synchrotron X-ray source recorded on an imaging plate with a monochromatic beam. The results strongly support the existence of a phase transformation of the hexagonal close-packed (hcp) structure to the new polymorph (β -phase of iron) at high pressure and temperature. We interpret the X-ray data as belonging to the double hexagonal close-packed (dhcp) structure distorted by stress due to laser heating. With the results of this study, we now have all reflections theoretically possible for the dhcp iron in d-spacing up to 1.15 Å.

We show the strong influence of deviatoric and thermal stresses on the results of lattice parameter determinations. The determination of exact lattice parameters of metals in laser heated DAC at high temperatures and pressures will require specially designed experiments in which stresses must be monitored carefully.

Acknowledgements We thank the Swedish Natural Science Research Council (NFR) for financial support. H.P. Weber thanks the Swiss National Science Foundation. The support of A Mazour at ID 30 is gratefully acknowledged.

References

- Anderson OL (1997) Iron: beta phase frays. *Science* 278:821–822
- Andrews KW (1955) X-ray diffraction by polycrystalline materials. Peiser HS, Roksby HP, Wilson AJC, (eds) London, pp 454–466
- Andrault D, Fiquet G, Kunz M, Visocekas F, Häusermann D (1977) The orthorhombic structure of iron: an *in situ* study at high-temperature and high-pressure. *Science* 278:831–834
- Belonoshko AB, Dubrovinsky LS (1997) A simulation study of induced failure and recrystallization of a perfect MgO crystal under non-hydrostatic compression. Application to melting in the diamond anvil cell. *Am Mineral* 82:441–451
- Berman BR (1976) Thermal conduction in solids, Oxford University Press, New York
- Boehler R (1993) Temperature in the Earth's core from melting-point measurements of iron at high pressures. *Nature* 363:534–536
- Dubrovinsky LS, Saxena SK, Lazor P (1997a) X-ray study of iron with *in-situ* heating at ultra high pressures. *Geophys Res Lett* 24:1835–1838
- Dubrovinsky LS, Saxena SK, Lazor P, Ahuja R, Eriksson O, Wills JM, Johansson B (1997b) Experimental and theoretical identification of a new high-pressure phase of silica. *Nature* 388:362–365
- Dubrovinsky LS, Saxena SK, Lazor P, Weber H-P (1998a) Structure of β -iron at high pressure and temperature. Technical comment, *Science* (in press)

- Dubrovinsky LS, Saxena SK, Lazor P (1998b) X-ray study of iron in electrically heated DAC at ultra high pressures. European Min J (in press)
- Duffy TS, Hemley RJ, Mao H-K (1995) Equation of state and shear strength at multimegabar pressures: magnesium oxide to 227 GPa. *Phys Rev Lett* 74:1371–1374
- Funamori N, Yagi T, Uchida T (1996) High-pressure and high-temperature *in situ* x-ray diffraction study of iron to above 30 GPa using MA8-type apparatus. *Geophys Res Lett* 23:953–956
- Heinz DL (1990) Thermal pressure in the laser-heated diamond anvil cell. *Geophys Res Letters* 17:1161–1164
- Keeler RN, Mitchell AC (1969) Electrical conductivity, demagnetization, and high-pressure phase transition in shock-compressed iron. *Solid State Commun* 7:271–274
- Kingma KJ, Cohen RE, Hemley RJ, Mao HK (1995) Transformation of stishovite to a denser phase at lower-mantle pressures. *Nature* 374:243–245
- Larson AC, Von Dreele RB (1994) *Los Alamos National Laboratory, LAUR*, 86–748
- Lazor P, Saxena SK (1996) Discussion comment on melting criteria and imaging spectroradiometry in laser-heated diamond-cell experiments. *Philos. Trans R Soc London, Ser A*, 354:1307–1313
- Li X, Manga M, Nguyen JH, Jeanloz R (1996) Temperature distribution in the laser-heated diamond cell with external heating, and implications for the thermal conductivity of perovskite. *Geophys Res Lett* 23:3775–3778
- Manga M, Jeanloz R (1997) Thermal conductivity of corundum and periclase and implications for the lower mantle. *J Geophys Res* 102:2999–3008
- Saxena SK, Shen G, Lazor P (1993a) Experimental evidence for new iron phase and implications for Earth's core. *Science* 260:1312–1314
- Saxena SK, Chatterjee N, Fei Y, Shen G (1993b) Thermodynamic data on oxides and silicates. Springer – Verlag, Berlin Heidelberg New York
- Saxena SK, Dubrovinsky LS, Häggkvist P, Cerenius Y, Shen G, Mao HK (1995) Synchrotron x-ray study of iron at high pressure and temperature. *Science* 269:1703–1704
- Saxena SK, Dubrovinsky LS, Häggkvist P (1996) X-ray evidence for the new phase β -iron at high temperature and high pressure. *Geophys Res Lett* 23:2441–2444
- Saxena SK, Dubrovinsky LS (1997) Detecting phases of iron. *Science* 275:94–96
- Shen G, Lazor P (1996) Measurement of melting temperatures of some minerals under lower mantle pressures. *J Geophys Res* 100:17699–17713
- Shen G, Mao H-K, Hemley RJ, Duffy T, Rivers ML (1998) Melting and crystal structure of iron at high pressures and temperatures. *Geophys Res Lett* 25:373–376
- Singh AK (1993) The lattice strains in specimen (cubic system) compressed nonhydrostatically in opposed anvil device. *J Appl Phys* 73:4278–4286
- Singh AK, Balasingh C (1994) The lattice strains in specimen (hexagonal system) compressed nonhydrostatically in opposed anvil device. *J Appl Phys* 75:4956–4962
- Söderlind PP, Moriarty JA, Willis JM (1996) First-principles theory of iron up to Earth core pressures: structural, vibrational and elastic properties. *Phys Rev B*, 53:14063–14072
- Touloukian YS, Ho CY (1971) Thermophysical properties of matter, vol 2, Macmillan, New York
- Yoo CS, Akella J, Campbell AJ, Mao HK, Hemley RJ (1995) Phase diagram of iron by *in situ* X-ray diffraction: implications for Earth's core. *Science* 270:1473–1475
- Yoo CS, Söderlind P, Campbell AJ (1996) DHCP as possible new ϵ' phase of iron at high pressure and temperature. *Phys Lett A* 214:65–68